J|A|C|S
ARTICLES
Published on Web 04/14/2007

Cisplatin Damage Overrides the Predefined Rotational Setting of Positioned Nucleosomes

Matthias Ober and Stephen J. Lippard*

Contribution from the Department of Chemistry, Massachusetts Institute of Technology, Cambridge, Massachusetts 02139

Received January 27, 2007; E-mail: lippard@mit.edu

Abstract: Cisplatin and carboplatin are used successfully to treat various types of cancer. The drugs target the nucleosomes of cancer cells and form intrastrand DNA cross-links that are located in the major groove. We constructed two site-specifically modified nucleosomes containing defined intrastrand *cis*-$\{Pt(NH_3)_2\}^{2+}$ 1,3-d(GpTpG) cross-links. Histones from HeLa-S3 cancer cells were transferred onto synthetic DNA duplexes having nucleosome positioning sequences. The structures of these complexes were investigated by hydroxyl radical footprinting. Employing nucleosome positioning sequences allowed us to quantify the structural deviation induced by the cisplatin adduct. Our experiments demonstrate that a platinum cross-link locally overrides the rotational setting predefined in the nucleosome positioning sequence such that the lesion faces toward the histone core. Identical results were obtained for two DNA duplexes in which the sites of platination differed by approximately half a helical turn. Additionally, we determined that cisplatin unwinds nucleosomal DNA globally by approximately 24°. The intrastrand *cis*-$\{Pt(NH_3)_2\}^{2+}$ 1,3-d(GpTpG) cross-links are located in an area of the nucleosome that contains locally overwound DNA in undamaged reference nucleosomes. Because most nucleosome positions *in vivo* are defined by the intrinsic DNA sequence, the ability of cisplatin to influence the structure of these positioned nucleosomes may be of physiological relevance.

Introduction

Cisplatin [*cis*-diamminedichloroplatinum(II)] and related agents such as carboplatin [*cis*-diammine(1,1′-cyclobutanedicarboxylato)platinum(II)] are among the few curative anticancer drugs. They are successfully used to treat various types of cancer, including testicular, ovarian, head, neck, and certain kinds of lung cancer.[1] Despite the benefit and success of platinum-based anticancer drugs, their application is limited by adverse characteristics including toxic side effects, the development of resistance after prolonged treatment, and effectiveness against a limited range of cancers.[1−3]

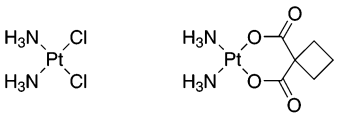

Cisplatin Carboplatin

A better understanding of the molecular mechanism of cisplatin action would assist in the design of chemotherapeutic drugs with improved efficacy. Cisplatin and carboplatin, which differ only by the nature of the leaving group, react with cellular DNA to form mainly intrastrand cross-links. The 1,3-d(GpXpG) *cis*-diammineplatinum(II) cross-links are the most abundant lesions produced by carboplatin, whereas 1,2-d(GpG) *cis*-diammineplatinum(II) adducts are preferred by cisplatin.[4]

DNA damage induced by platinum-based drugs has been investigated mainly with the use of purified DNA. In a cellular environment, however, DNA is compacted in highly condensed chromatin structures, the fundamental building blocks of which are the nucleosomes. Cisplatin reacts with this nucleosomal DNA as well as with free DNA,[5] but the former is the more likely target *in vivo*. It is therefore of interest to determine the effect of platinum damage in the context of the nucleosome. The properties of nucleosomes containing various DNA lesions, including *N*-methylpurines[6] and the TT cyclobutane pyrimidine dimer,[7−11] have been previously investigated. Recently work in our laboratory using hydroxyl radical footprinting experiments showed that a defined 1,3-d(GpTpG) platinum adduct in nucleosomal DNA lacking a strong positioning sequence induces a particular rotational setting of the DNA on the histone core.[12]

(1) Wong, E.; Giandomenico, C. M. *Chem. Rev.* **1999**, *99*, 2451−2466.
(2) Jamieson, E. R.; Lippard, S. J. *Chem. Rev.* **1999**, *99*, 2467−2498.
(3) Wang, D.; Lippard, S. J. *Nat. Rev. Drug Discovery* **2005**, *4*, 307−319.
(4) Blommaert, F. A.; van Dijk-Knijnenburg, H. C. M.; Dijt, F. J.; den Engelse, L.; Baan, R. A.; Berends, F.; Fichtinger-Schepman, A. M. J. *Biochemistry* **1995**, *34*, 8474−8480.
(5) Lippard, S. J.; Hoeschele, J. D. *Proc. Natl. Acad. Sci. U.S.A.* **1979**, *76*, 6091−6095.
(6) Li, S. S.; Smerdon, M. J. *J. Biol. Chem.* **2002**, *277*, 44651−44659.
(7) Kosmoski, J. V.; Ackerman, E. J.; Smerdon, M. J. *Proc. Natl. Acad. Sci. U.S.A.* **2001**, *98*, 10113−10118.
(8) Svedružić, Ž. M.; Wang, C.; Kosmoski, J. V.; Smerdon, M. J. *J. Biol. Chem.* **2005**, *280*, 40051−40057.
(9) Thoma, F. *EMBO J.* **1999**, *18*, 6585−6598.
(10) Schieferstein, U.; Thoma, F. *EMBO J.* **1998**, *17*, 306−316.
(11) Schieferstein, U.; Thoma, F. *Biochemistry* **1996**, *35*, 7705−7714.
(12) Danford, A. J.; Wang, D.; Wang, Q.; Tullius, T. D.; Lippard, S. J. *Proc. Natl. Acad. Sci. U.S.A.* **2005**, *102*, 12311−12316.

10.1021/ja0706145 CCC: $37.00

Scheme 1. Construction of Site-Specifically Platinated Nucleosome Positioning Sequences

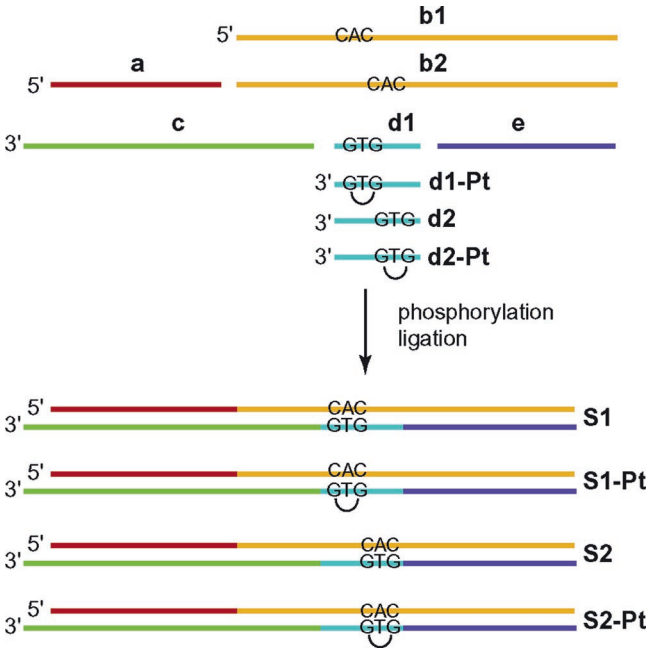

In that study, recombinant rather than native histones were used to reconstitute the platinum-damaged nucleosomes.

One principal aim of the work reported here was to determine whether the presence of a *cis*-$\{Pt(NH_3)_2\}^{2+}$ 1,3-d(GpTpG) intrastrand cross-link would be sufficiently strong to influence the setting of nucleosomal DNA containing a predefined positioning sequence. More than 50% of the nucleosome positions in *Saccharomyces cerevisiae* can be explained by the underlying DNA sequence through a model that takes into account steric hindrance and competition between nucleosomes.[13,14] Positioned nucleosomes perform important regulatory functions, such as attenuating or increasing gene expression,[13] and fulfill structural tasks, such as protection of the centromere region.[14] It is possible to obtain detailed structural information about positioned nucleosome particles by hydroxyl radical footprinting.[15] Comparison of selectively platinated with sequence-identical unplatinated reference nucleosomes will allow a precise quantification of the structural deviation induced by the cisplatin adduct, and obtaining this information was the second goal of this study.

The nucleosomes in the present study were reconstituted by using histones from chromatin donated by HeLa-S3 cancer cells rather than recombinant histones. Histones in eukaryotic cells are subjected to a diverse array of physiologically important posttranslational modifications,[16] which differentiates them from recombinant histones. We were therefore interested, as the third major objective, to learn whether or not such modifications would influence the positioning effect of the 1,3-d(GpTpG) cisplatin lesion relative to the nucleosome histone core.

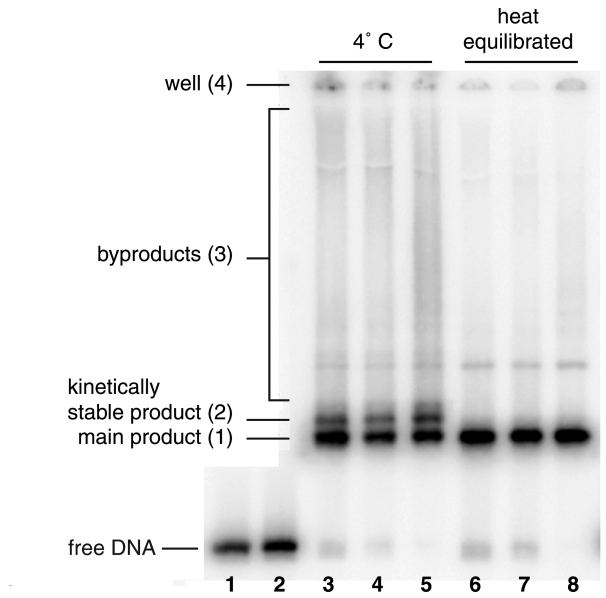

Figure 1. Product distributions from the histone transfer reaction onto the **S1** duplex. Lanes 1 and 2, free DNA; lanes 3−5, after completion of transfer reactions at 4 °C; lanes 6−8, after heat equilibration at 45 °C/2 h. The average length of donor chromatin: lanes 3 and 6, 750 bp; lanes 4 and 7, 450 bp; lanes 5 and 8, 250 bp.

Results and Discussion

Design of DNA Sequences. The choice of the DNA sequence for duplex **S1-Pt** was based on that in the strongly positioned 145-base pair (bp) pD89 nucleosome.[17] The DNA was constructed with a 3′ overhang of 9 bp to facilitate ligation in future experiments and contains a site-specific *cis*-$\{Pt(NH_3)_2\}^{2+}$ 1,3-d(GpTpG) cross-link. The sequence of **S2-Pt** is identical to that of **S1-Pt**, except for a shift of the platinum cross-link by 5 bp to the 5′-direction of the platinated strand. Both duplexes were prepared by enzymatic ligation of synthetic oligonucleotides, as shown in Scheme 1. As a reference, the corresponding unplatinated duplexes **S1** and **S2** were also prepared. The fragments and complete sequences are provided in Scheme S1 (Supporting Information).

Histone Transfer to DNA Containing Site-Specific Cisplatin Lesions. Low-molecular-weight chromatin with an average length of 750 bp (3−5 nucleosomes), 450 bp (2−3 nucleosomes), or 250 bp (1−2 nucleosomes) was prepared from HeLa-S3 cells as described in the Experimental Section. All donor chromatin samples were tested in transfer reactions with **S1**, **S1-Pt**, **S2**, and **S2-Pt**, employing microdialysis. In addition, we investigated the effect of heat equilibration[18,19] on product composition. Four different types of product were observed by native gel electrophoresis studies (Figure 1): (1) a main band containing positioned, thermodynamically stable nucleosomes; (2) a band containing a nucleosome conformation that is kinetically stabilized at 4 °C but disappears after heat equilibration; (3) nucleosomes with no defined DNA position and aggregates thereof; and (4) a residue that remained in the well, presumed to be high-molecular-weight aggregates. Complete

(13) Ioshikhes, I.; Bolshoy, A.; Derenshteyn, K.; Borodovsky, M.; Trifonov, E. N. *J. Mol. Biol.* **1996**, *262*, 129−139.
(14) Segal, E.; Fondufe-Mittendorf, Y.; Chen, L.; Thåström, A.; Field, Y.; Moore, I. K.; Wang, J.-P. Z.; Widom, J. *Nature* **2006**, *442*, 772−778.
(15) Hayes, J. J.; Tullius, T. D.; Wolffe, A. P. *Proc. Natl. Acad. Sci. U.S.A.* **1990**, *87*, 7405−7409.
(16) Jenuwein, T.; Allis, C. D. *Science* **2001**, *293*, 1074−1080.
(17) Studitsky, V. M.; Clark, D. J.; Felsenfeld, G. *Cell* **1994**, *76*, 371−382.
(18) Dyer, P. N.; Edayathumangalam, R. S.; White, C. L.; Bao, Y. H.; Chakravarthy, S.; Muthurajan, U. M.; Luger, K. *Methods Enzymol.* **2004**, *375*, 23−44.
(19) Pennings, S. *Methods Enzymol.* **1999**, *304*, 298−312.

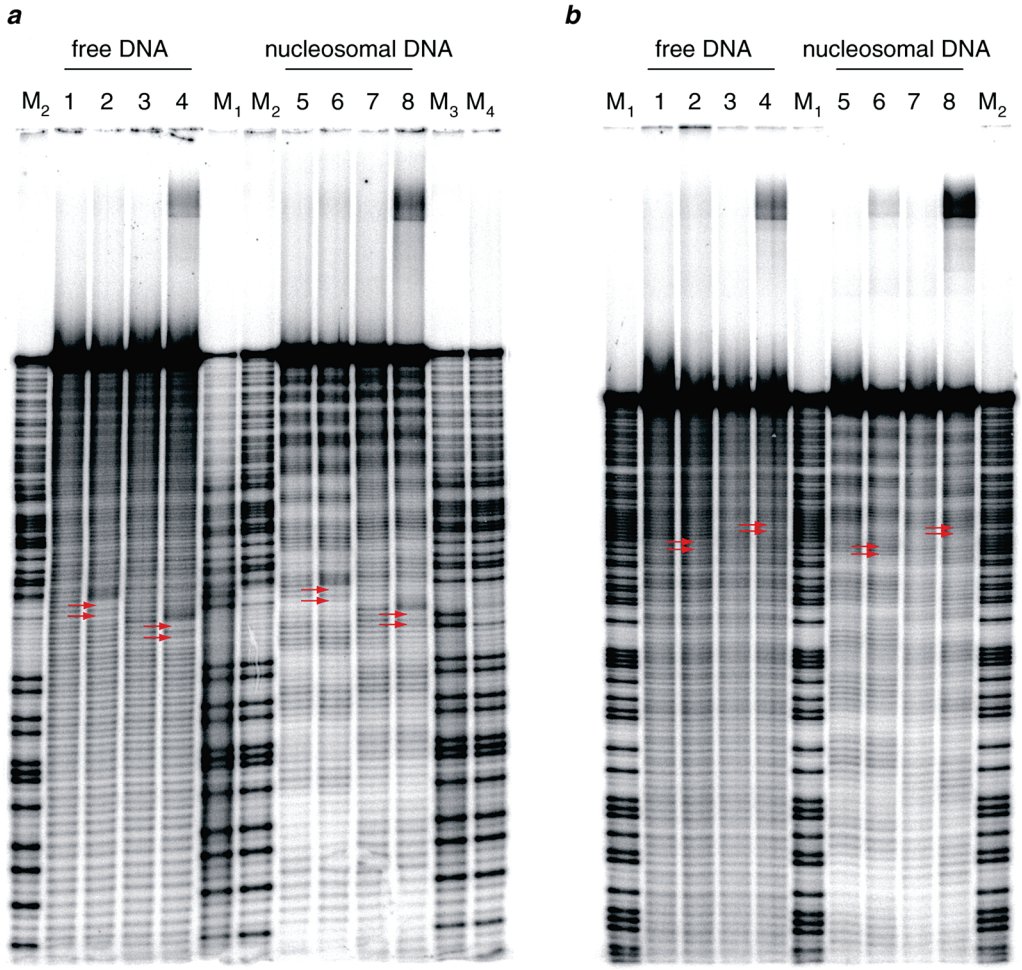

Figure 2. Autoradiographs of footprinting experiments. (a) The template strands of the duplexes were 5′-labeled with ^{32}P. The positions of the platinum adduct are highlighted by red arrows. Lane 1, **S1**; lane 2, **S1-Pt**; lane 3, **S2**; lane 4, **S2-Pt**; lane 5, **nS1**; lane 6, **nS1-Pt**; lane 7, **nS2**; lane 8, **nS2-Pt**; lane M_1, Maxam−Gilbert A/G reaction of **S1**; lane M_2, Maxam−Gilbert A/G reaction of **S1-Pt**; lane M_3, Maxam−Gilbert A/G reaction of **S2**; lane M_4, Maxam−Gilbert A/G reaction of **S2-Pt**. (b) The coding strands of the duplexes were 5′-labeled. The positions of the d(CpApC) trinucleotide opposite the platinum adduct are highlighted by red arrows. Lane 1, **S1**; lane 2, **S1-Pt**; lane 3, **S2**; lane 4, **S2-Pt**; lane 5, **nS1**; lane 6, **nS1-Pt**; lane 7, **nS2**; lane 8, **nS2-Pt**; lanes M_1, Maxam−Gilbert A/G reaction of **S1**; lane M_2, Maxam−Gilbert A/G reaction of **S2**.

autoradiographs and the results of this experiment are detailed in Figure S1 (Supporting Information).

The donor chromatin length distribution did not significantly influence the overall transfer yield but did affect the fraction of desired main product (1, above). Donor chromatin with an average length of 1−2 nucleosomes gave a larger fraction of undefined nucleosomes and aggregates. The use of higher molecular weight donor chromatin (3−5 nucleosomes) typically increased the amount of product that remained in the wells (4, above). The highest transfer yields onto platinum-damaged DNA occurred with donor chromatin having an average length of >2 nucleosomes. The kinetically stabilized nucleosome conformation (2, above) was only formed in significant amounts (15−20%) in transfer reactions onto unplatinated DNA. Sequence-induced DNA curvature is the major factor that determines the rotational and translational setting of nucleosomal DNA.[20] The structural influence of a cisplatin lesion on overall DNA curvature[21−24] may be responsible for this effect.

Transfer mixtures that were heat equilibrated after dialysis contained around 90% of positioned nucleosomes, irrespective of donor chromatin length. The rotational settings of the nucleosomal DNA in the main band before and after heat equilibration were identical, as established by footprinting experiments (see below).

Footprinting of Cisplatin-Damaged Nucleosomes. We prepared the nucleosomes **nS1**, **nS1-Pt**, **nS2**, and **nS2-Pt** from the respective DNA duplexes **S1**, **S1-Pt**, **S2**, and **S2-Pt** by using donor chromatin with an average length of 2−3 nucleosomes and subsequent heat equilibration. They were analyzed by hydroxyl radical footprinting experiments.[25,26] In order to examine the positions of the two strands of the DNA duplex relative to the histone octamer core in the nucleosome, we conducted separate experiments in which either the template or the coding strand was labeled with ^{32}P. As a reference, both strands of the free DNA duplexes **S1**, **S1-Pt**, **S2**, and **S2-Pt**

(20) Lowary, P. T.; Widom, J. *J. Mol. Biol.* **1998**, *276*, 19−42.
(21) Bellon, S. F.; Coleman, J. H.; Lippard, S. J. *Biochemistry* **1991**, *30*, 8026−8035.
(22) Cohen, G. L.; Bauer, W. R.; Barton, J. K.; Lippard, S. J. *Science* **1979**, *203*, 1014−1016.
(23) Rice, J. A.; Crothers, D. M.; Pinto, A. L.; Lippard, S. J. *Proc. Natl. Acad. Sci. U.S.A.* **1988**, *85*, 4158−4161.
(24) Van Garderen, C. J.; Van Houte, L. P. A. *Eur. J. Biochem.* **1994**, *225*, 1169−1179.
(25) Dixon, W. J.; Hayes, J. J.; Levin, J. R.; Weidner, M. F.; Dombroski, B. A.; Tullius, T. D. *Methods Enzymol.* **1991**, *208*, 380−413.
(26) Vitolo, J. M.; Thiriet, C.; Hayes, J. J. *Curr. Protoc. Mol. Biol.* **1999**, 21.4.1−21.4.9.

were also studied by footprinting. The autoradiographs obtained by analysis of the sequencing gels are shown in Figure 2. Expanded versions are presented in Figure S2 (Supporting Information), and aligned densitometric scans of these autoradiographs together with the sequence assignments are presented in Figures S3 and S4 (Supporting Information). Between 110 and 120 individual nucleotides were resolved at 1-bp resolution. It was possible to correlate each band with the corresponding sequence with the aid of Maxam−Gilbert A/G sequencing reference lanes. The positions of cisplatin adducts are indicated by missing double bands in the Maxam−Gilbert density traces after superposition of the traces of **S1** and **S1-Pt** or **S2** and **S2-Pt**, respectively.

The traces in Figure 2a,b, lanes 1−4, represent the footprinting patterns of the unbound duplexes. Because the backbones of these strands are exposed to hydroxyl radicals in an approximately isotropic fashion, an even fragmentation pattern is produced. Purine nucleotides are slightly more sensitive to radical cleavage and autoradiolysis and give stronger signals than pyrimidine nucleotides.[26,27] Also displayed are the traces of the four reconstituted nucleosomes, lanes 5−8. The periodic intensity modulation in the footprinting pattern reflects the helical structure of the DNA packed against the histone octamer core proteins. Hydroxyl radicals react preferentially with the C5′-hydrogen atoms of the sugar−phosphate backbone.[28] The backbone is therefore preferentially cleaved at solvent-exposed regions facing away from the histone core. This preferential cleavage results in darker bands. Regions in which the sugar−phosphate backbone faces the histone core are less likely to be cleaved and produce lighter bands. The intensity of each band was resolved by deconvolution. The data were used to determine cleavage curves that indicate the solvent exposure of the backbone at each nucleotide, from which detailed structural information about the nucleosomal DNA could be derived. By overlaying the cleavage curves of both strands in a duplex, it was possible to identify the disposition of the major and minor grooves of the nucleosomal DNA relative to the histone core. In order to describe the orientation of the major groove at a given base pair relative to the histone octamer surface, we define an angle ξ (details in Supporting Information; see also below), which approximates 0° if the major groove faces toward the histone core and 180° if it points to the solvent-exposed nucleosome surface.

Structural Consequences of the *cis*-{Pt(NH$_3$)$_2$}$^{2+}$ 1,3-d(GpTpG) Cross-Link. The position of the platinum lesion defines the rotational setting of the nucleosomal DNA and overrides the preference as defined by the nucleosome positioning sequence. Three factors were identified that contribute to and reveal this conformational effect. First, moving the d(GpTpG) trinucleotide itself by half a helical turn alters the rotational setting globally by 30−70°. This result is clear from the footprinting patterns of the unplatinated nucleosomes **nS1** and **nS2**, which are out of phase by 1−2 bp (Figure 3a).

Second, the platinum adduct, which is always located in the major groove,[2] rotates the DNA duplex locally in such a manner that the lesion faces toward the histone core ($\xi \approx 0°$). This effect is visible in the cleavage curves of both the template and the coding strands of the nucleosomal DNA. In **nS1** nucleosomes, the major groove of the DNA at the d(GpTpG) trinucleotide already has this orientation (Figure 4a). In this case, the presence of the cisplatin adduct in the **nS1-Pt** nucleosome does not induce a major conformation change of the DNA when compared to the **nS1** nucleosome (Figure 4c). For the **nS2** nucleosomes, in which the d(GpTpG) trinucleotide is shifted by 5 bp, the major groove is oriented at $\xi \approx 90°$ with respect to the histone octamer (Figures 4b and 5a). Addition of the cisplatin adduct in **nS2-Pt** nucleosomes induces a local twist of the DNA at the d(GpTpG) site by approximately 90°. The cisplatin adduct again faces toward the histone core (Figures 4d and 5b). This twist causes local underwinding of the DNA 5′ to the cisplatin adduct and local overwinding 3′ to the adduct, as shown in the periodicity plots that were calculated from the cleavage curves. The combined two effects result in a change of the rotational setting by almost 180° when the *cis*-{Pt(NH$_3$)$_2$}$^{2+}$ 1,3-d(GpTpG) cross-link is shifted by 5 bp. The cleavage curves of the **nS1-Pt** and **nS2-Pt** nucleosomes exhibit a phase difference of approximately 180° in the region of the cisplatin lesion and the directly adjacent helical turns. More remote from the cisplatin adduct, the phase difference gradually decreases to just a quarter turn (Figure 3b).

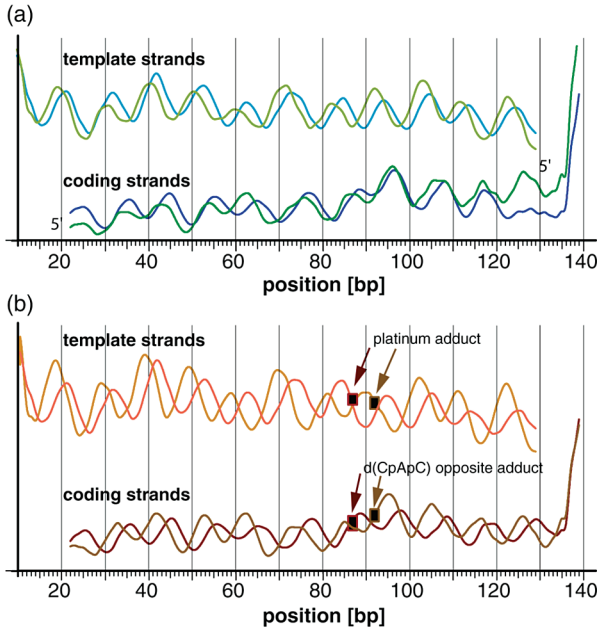

Figure 3. Superimposition of the cleavage curves of (a) unplatinated and (b) platinated nucleosomes. (a) The DNA sequences of the unplatinated nucleosomes **nS1** (blue) and **nS2** (green) are identical except for the fact that a d(GpTpG) trinucleotide in the bottom strand was shifted by 5 bp. The corresponding cleavage curves are out of phase by 1−2 bp. (b) The platinated nucleosomes **nS1-Pt** (red) and **nS2-Pt** (orange) have identical sequences except for the fact that the 1,3-d(GpTpG) cisplatin adduct, symbolized by a black rectangle, was shifted by 5 bp. The corresponding cleavage curves are out of phase by 3−5 bp. The phasing difference is almost 180° in the vicinity of the cisplatin adduct.

Third, the d(GpTpG) cisplatin adduct unwinds the nucleosomal DNA duplex globally. This effect can be visualized by superimposing cleavage curves for the DNA of **nS1** and **nS1-Pt** nucleosomes. Figure 6 reveals that the cleavage curve 3′ to the d(GpTpG) adduct is almost congruent with the curve of the reference strand. On the 5′ side of the adduct, the curves are out of phase by approximately 1 bp.

To quantify the global unwinding effect more accurately, the mean periodicities of the nucleosomes **nS1**, **nS1-Pt**, **nS2**, and

(27) Burrows, C. J.; Muller, J. G. *Chem. Rev.* **1998**, *98*, 1109−1151.
(28) Balasubramanian, B.; Pogozelski, W. K.; Tullius, T. D. *Proc. Natl. Acad. Sci. U.S.A.* **1998**, *95*, 9738−9743.

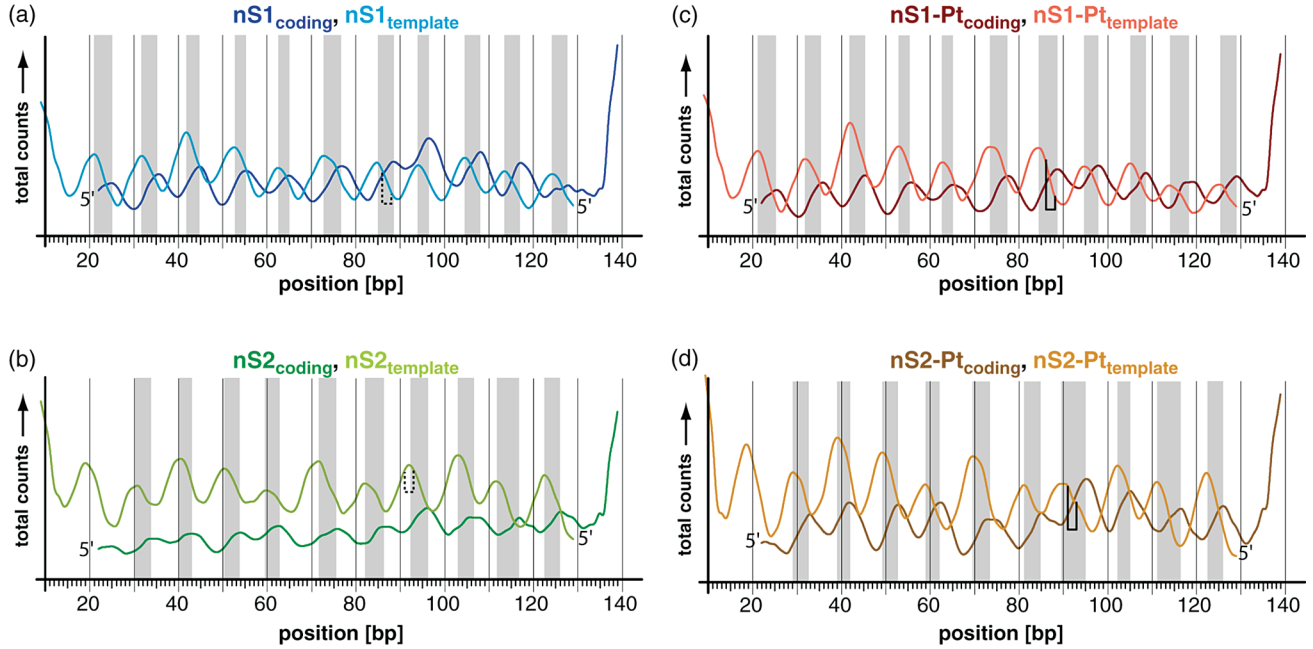

Figure 4. The cleavage curves reveal the rotational setting of the nucleosomal duplexes **nS1**, **nS1-Pt**, **nS2**, and **nS2-Pt** in the nucleosome. Gray bars indicate areas in which the minor groove is exposed to the solvent and the major groove faces inward to the nucleosome. (a) The major groove of the unplatinated d(GpTpG) trinucleotide of **S1** faces inward. (b) The major groove of the unplatinated d(GpTpG) site of **nS2** faces sideways. (c,d) The major groove of the platinated d(GpTpG) sites faces inward in both cases. Cisplatin, which binds to the purine bases in the major groove of DNA, is in both cases buried inside the nucleosome, inaccessible to the solvent.

nS2-Pt were determined. For the unplatinated nucleosomes **nS1** and **nS2**, periodicities of $n = 10.32 \pm 0.05$ bp and $n = 10.27 \pm 0.06$ bp, respectively, were determined. These values correspond well with the previously reported periodicity of 10.2 bp for nucleosomal DNA.[15,29] The platinated nucleosomes **nS1-Pt** and **nS2-Pt** have mean helical periodicities of $n = 10.38 \pm 0.05$ bp and $n = 10.33 \pm 0.05$ bp, respectively. The difference in the mean values in both cases is 0.06, which corresponds to a global duplex unwinding of 0.67 ± 0.08 bp or $24 \pm 3°$; 11 complete helical turns were resolved for all nucleosomes. Previous NMR analysis and electrophoresis studies showed that the 1,3-d(GpTpG) cisplatin cross-link unwinds free DNA strands by 19−23°.[21,24] Cisplatin unwinds nucleosomal DNA by precisely the same amount.

Helical Periodicities, Symmetry, and Translational Position. The helical periodicity of DNA in the nucleosome is not constant but changes within the particle. For 5S *Xenopus borealis* DNA, hydroxyl radical footprinting experiments showed that a 30-bp region around the center of pseudodyad symmetry has an average periodicity of around $n = 10.7$ bp, whereas the remaining strands farther from the pseudodyad axis have a periodicity of $n = 10.05$.[15] Essentially the same effect was observed here. The average periodicities of the 30-bp central region are $n = 10.6$, 10.8, 10.8, and 10.5 for **nS1**, **nS1-Pt**, **nS2**, and **nS2-Pt**, respectively, while the remaining DNA has a periodicity of $n = 10.2$, 10.2, 10.0, and 10.2, respectively (Table S2, Supporting Information). Thus, helical periodicity is not constant for the platinum-damaged nucleosomal DNA. A symmetric change in helix periodicity is clearly visible in the periodicity plots (Figure 7). Two minor peaks flank a central peak symmetrically at a distance of about 26 bp, or one-third of a turn around the nucleosome.

For reasons of symmetry, we assume that the central peak with the highest periodicity corresponds to the position of the pseudodyad axis. This method allows us to estimate the translational setting of positioned nucleosomes directly by hydroxyl radical footprinting and avoids any ambiguity that may be introduced by the more indirect exonuclease III mapping protocol.[12]

Shifting the unplatinated d(GpTpG) trinucleotide by 5 bp causes a measurable shift in the observed helical periodicities. Moving d(GpTpG) in the duplex from position 86.88 in **nS1** to 91.93 in **nS2** shifts the entire periodicity curve by about 3 bp in the opposite direction. The central peak at position 75 moves to position 72, while the relative distance between all peaks remains identical. Addition of a cisplatin 1,3-intrastrand cross-link, however, has no influence on the position of the center and flanking peaks.

A variety of footprinting studies[15,30,31] describe such symmetric behavior and a local increase in periodicity around the pseudodyad axis. Crystal structures of the nucleosome core particle, on the other hand, show an asymmetry in the setting of the DNA duplex and a much smaller change in helical periodicity throughout the nucleosome core particle.[29,32] The reason for this discrepancy is not yet fully understood.[33]

Comparative crystallographic studies suggest that DNA overwinding, which is accompanied by DNA stretching and narrowing of the minor groove, is only possible and observed in certain regions of the nucleosomes.[32] These regions are about ±2 and ±5 full helical turns away from the pseudodyad axis.

(29) Luger, K.; Mäder, A. W.; Richmond, R. K.; Sargent, D. F.; Richmond, T. J. *Nature* **1997**, *389*, 251−260.
(30) Bryan, P. N.; Wright, E. B.; Olins, D. E. *Nucleic Acids Res.* **1979**, *6*, 1449−1465.
(31) Klug, A.; Lutter, L. C. *Nucleic Acids Res.* **1981**, *9*, 4267−4283.
(32) Muthurajan, U. M.; Park, Y. J.; Edayathumangalam, R. S.; Suto, R. K.; Chakravarthy, S.; Dyer, P. N.; Luger, K. *Biopolymers* **2003**, *68*, 547−556.
(33) Negri, R.; Buttinelli, M.; Panetta, G.; De Arcangelis, V.; Di Mauro, E.; Travers, A. *Biochem. Soc. Trans.* **2000**, *28*, 373−376.

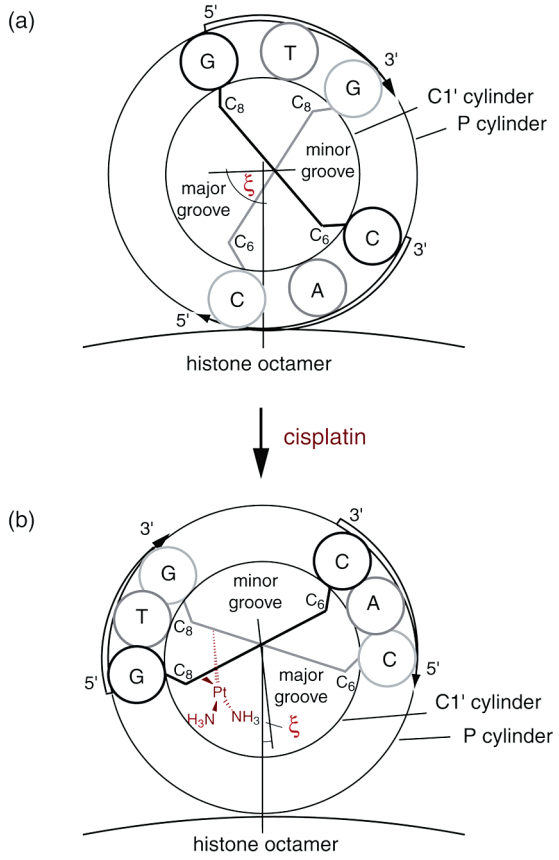

Figure 5. Schematic projection of the d(GpTpG) trinucleotide (position 91.93) of the nucleosomes (a) **nS2** and (b) **nS2-Pt** along the central axis of the nucleosomal DNA. The two concentric circles indicate expected locations of the P- and C1′-atoms in the DNA duplex. The G:C base pairs are symbolized by thick lines. (a) The major groove of the unplatinated d(GpTpG) trinucleotide points sideways ($\xi \approx 90°$) and its backbone faces directly to the solvent. (b) The major groove of the d(GpTpG) trinucleotide and the platinum adduct point toward the histone octamer ($\xi \approx 0°$) and its minor groove faces directly toward the solvent.

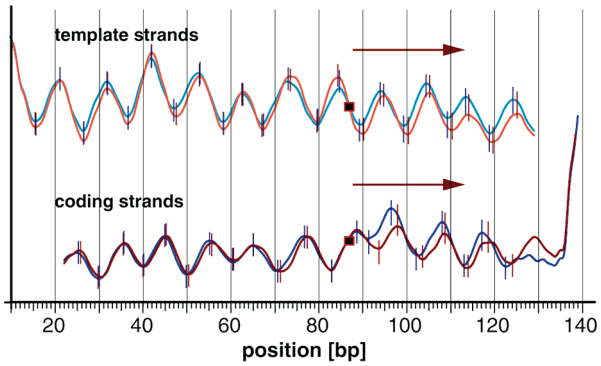

Figure 6. Superimposition of the cleavage curves of the unplatinated nucleosome **nS1** and the corresponding platinated nucleosome **nS1-Pt** shows that the cisplatin adduct unwinds the DNA strand on the nucleosome by approximately 1 bp.

It has been suggested that intercalating and DNA-unwinding agents would therefore be preferably accommodated in areas located either ±2 or ±5 full helical turns away from the pseudodyad axis.[32] We note that the DNA-unwinding cisplatin lesion in both nucleosomes studied here is located in a region that is locally overwound. The position of cisplatin is about 1.5 helical turns for **nS1** or 2.5 helical turns for **nS2** away from the position that we have identified as the pseudodyad axis.

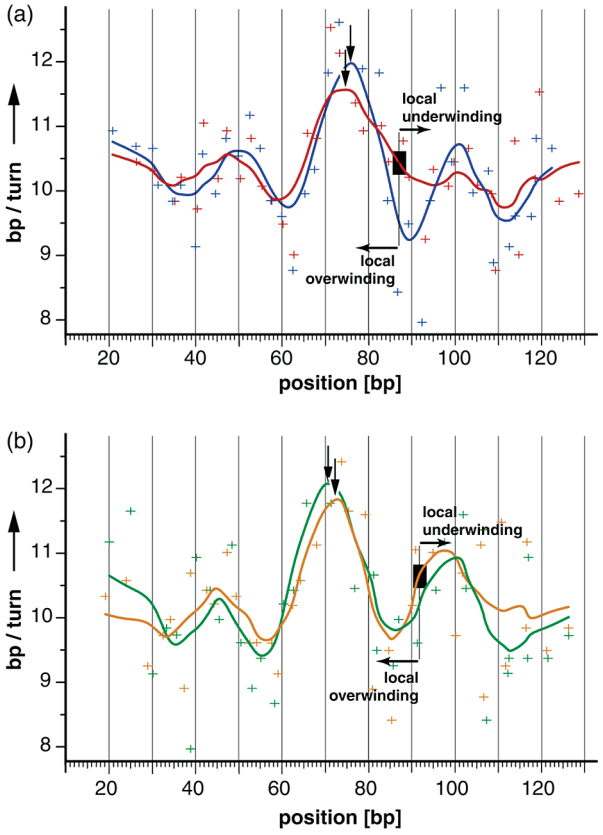

Figure 7. Helical periodicities of nucleosomal DNA strands: (a) **n1S** (blue) and **n1S-Pt** (red) superimposed; (b) **n2S** (green) and **n2S-Pt** (orange) superimposed. The positions of the platinum cross-links are indicated by black rectangles and the pseudodyad axes by arrows. Comparison of platinated and unplatinated nucleosomes reveals a local underwinding and overwinding in the vicinity of the cisplatin adduct.

Comparison to Related Studies. The present results reinforce and significantly augment our previously communicated findings.[12] In that study we reported that a 1,3-d(GpTpG) cisplatin intrastrand cross-link defines the rotational and translational position of a random DNA sequence that was wrapped around a nucleosome reconstituted with recombinant histones. The random, platinum-free DNA sequence did not enforce a defined nucleosomal position and gave no clear intensity modulation pattern. Addition of *cis*-$\{Pt(NH_3)_2\}^{2+}$ intrastrand 1,3-d(GpTpG) cross-links defined the rotational and translational position of the nucleosomal DNA. Similarly, the cisplatin adduct turned away from the solvent-exposed side and toward the core of the nucleosome particle. The present work has two major distinctions. First, instead of recombinant histones, donor chromatin from human cancer cells was used to reconstitute the sample nucleosomes. These histones bear a variety of posttranslational modifications,[16] and it was important to investigate whether they influence the positioning capability of the cisplatin adduct. In our present study, we discovered that global posttranslational modifications do not alter the positioning ability of the 1,3-d(GpTpG) cisplatin lesion. Moreover, significant advantages of the histone transfer protocol used here are its high reproducibility and generally very high yields.

Second, instead of a random DNA sequence, we employed a strongly positioning DNA sequence. Positioned nucleosomes are common, with the majority of nucleosomes *in vivo* seeming

to be well-positioned.[34] The genomic sequence defines the location of at least 50% of all nucleosomes.[14] Characteristic nucleosome positioning patterns are particularly encountered in promoter regions and at translation start sites,[13,14,35] indicating that positioned nucleosomes regulate gene transcription. The ability of the cisplatin to alter predefined rotational settings within nucleosome positioning sequences may therefore play an important role in determining the physiological consequences of the drug.

The positioning sequence helped us to obtain detailed structural information about both the platinated DNA strands and the unplatinated reference strands. It was possible to quantify the structural deviations induced by the cisplatin adduct in an accurate manner. The rotational setting of nucleosomal DNA *in vivo* is mainly influenced by a sequence-induced DNA bending. This bending is caused by subtle collective effects of certain dinucleotide steps at specific positions.[14,36] The 1,3-d(GpTpG) platinum adduct induces a 30° kink toward the major groove of the DNA,[37] the geometric consequences of which are probably the key reason for the strong positioning potential of the cisplatin lesion.

Summary and Conclusions

Nucleosomes containing site-specific 1,3-d(GpTpG) cisplatin intrastrand cross-links have been reconstituted using DNA with a strong nucleosome positioning sequence and histones from human HeLa-S3 cell chromatin. A variety of factors influence the position of a 1,3-d(GpTpG) platinum adduct within these synthetic nucleosomes, as revealed by hydroxyl radical footprinting. Moving the d(GpTpG) trinucleotide itself alters the rotational setting by 30−70°. The platinum cross-link enhances that effect by twisting the DNA such that the adduct faces the histone core. Shifting a 1,3-d(GpTpG) intrastrand cross-link by 5 base pairs causes a 180° rotation of the DNA close to that area and overrides the rotational setting predefined by a nucleosome positioning sequence. The use of native rather than recombinant histones has no influence on the ability of the cisplatin adduct to define the rotational setting of the DNA on the histone core. The platinum lesion induces local underwinding of the DNA to the 5′ direction and overwinding to the 3′ direction. In addition, cisplatin unwinds nucleosomal DNA by approximately 0.67 bp or 24°, similar to the value observed for free DNA bearing the same lesion.[21,24] These results have elevated our understanding of the effects of cisplatin−DNA damage to the level of the nucleosome, the fundamental building block of our genome.

Experimental Section

Materials and Methods. Chemical reagents and solvents were purchased from commercial sources. $K_2[PtCl_4]$ was received as a gift from Engelhard Corp. (Iselin, NJ, now BASF). Cisplatin was synthesized from $K_2[PtCl_4]$ according to a published procedure.[38] γ-^{32}P-ATP having a specific activity of at least 6000 Ci/mmol was obtained from Perkin-Elmer (Boston, MA). DNA synthesis was conducted on an Applied Biosystems 392 DNA/RNA synthesizer on a 1 μmol scale by using a standard phosphoramidite protocol. The oligonucleotides were deprotected overnight at 60 °C and dried with an Eppendorf Vacufuge. Chromatographic analysis and preparative high-performance liquid chromatography (HPLC) purification of oligonucleotides was performed on a HP Waters system using GraceVydac 10 × 250 mm C18 columns (particle/pore size of 10 μm/30 nm). Buffer A contained 0.1 M tetraethylammonium acetate in water, and buffer B contained 0.1 M tetraethylammonium acetate in 80% (v/v) acetonitrile. The r_b values, moles of Pt bound per nucleotide residue, were determined by quantification of platinum using flameless atomic absorption spectrophotometry (Perkin-Elmer AAnalyst 300 system) and DNA by UV/vis spectroscopy (Cary 1E spectrometer from Varian). The specific extinction coefficient of each oligonucleotide was estimated as the sum of the individual extinction coefficients of the nucleotides in the sequence.[39,40] Matrix-assisted laser desorption/ionization (MALDI) measurements were conducted on a Bruker Omniflex mass spectrometer at the Department of Chemistry Instrumentation Facility (Massachusetts Institute of Technology) or on an Applied Biosystems Voyager DE-STR mass spectrometer at the MIT CCR Biopolymers Laboratory. Enzymes were obtained from New England Biolabs (Ipswich, MA) unless otherwise specified. Enzymatic reactions were carried out in reaction buffers provided with the enzyme unless otherwise noted. Pelleted HeLa-S3 cells were obtained from the National Cell Culture Center (Minneapolis, MN). Beckmann-Coulter Avanti J-25 or Optima L centrifuges were used for chromatin preparation. For chromatin sonication, a Branson digital sonifier was utilized. All steps involving proteins, such as chromatin isolation, purification, and histone transfer, were carried out at 4 °C or on ice if not otherwise noted. Dialysis membranes were obtained from Spectra/Por and treated with hot 50 mM EDTA solution, followed by several washes with high-purity water with a conductivity of >12 MΩ, before use to remove trace divalent cations. Denaturing DNA polyacrylamide gel electrophoresis (PAGE) was performed on a Life Technologies S2 sequencing gel electrophoresis apparatus. For native DNA and nucleosome gel electrophoresis, a Protean II xi cell from BioRad was used. Fluorescent agarose electrophoresis gels were documented on a BioRad Fluor-S MultiImager. Electrophoresis gels with radioactive samples were dried and documented on a Storm 840 Phosphorimager system from Amersham or exposed wet to a Kodak Biomax MS film. Radioactive samples were quantified on a Beckman LS 6500 scintillation counter. Fast protein liquid chromatography was performed with a system from Amersham (P1 peristaltic pump and a programmable Frac-100 fraction collector).

Synthesis of Platinated Oligonucleotides. First, seven oligonucleotides, **a**, **b1**, **b2**, **c**, **d1**, **d2**, and **e**, the sequences of which are provided in Scheme S1a (Supporting Information), were chemically synthesized and purified by preparative PAGE in the presence of 7.5 M urea. The oligonucleotides were ethanol precipitated and desalted with SepPak C18 cartridges. The purified strands were characterized by MALDI-TOF mass spectrometry and quantified by UV/vis spectroscopy. The two 14-mer oligonucleotides **d1** and **d2** were converted into **d1-Pt** and **d2-Pt** by introduction of specific *cis*-$\{Pt(NH_3)_2\}^{2+}$ 1,3-d(GpTpG) intrastrand cross-links according to published procedures.[41] The platinated strands were purified by semipreparative HPLC, and the quality of the fractions was monitored by analytical HPLC. The pure fractions were pooled and concentrated by ethanol precipitation. The r_b values of the obtained 14mers **d1-Pt** and **d2-Pt** were determined to be 1.03/14 and 1.06/14, respectively, corresponding to one cisplatin adduct per oligonucleotide.

Preparation and Characterization of DNA Duplexes. The oligonucleotides **b1**, **b2**, **c**, **d1**, **d1-Pt**, **d2**, and **d2-Pt** were 5′-phosphorylated

(34) Yuan, G. C.; Liu, Y. J.; Dion, M. F.; Slack, M. D.; Wu, L. F.; Altschuler, S. J.; Rando, O. J. *Science* **2005**, *309*, 626−630.
(35) Ercan, S.; Lieb, J. D. *Nat. Genet.* **2006**, *38*, 1104−1105.
(36) Satchwell, S. C.; Drew, H. R.; Travers, A. A. *J. Mol. Biol.* **1986**, *191*, 659−675.
(37) Teuben, J.-M.; Bauer, C.; Wang, A. H.-J.; Reedijk, J. *Biochemistry* **1999**, *38*, 12305−12312.
(38) Dhara, S. C. *Indian J. Chem.* **1970**, *8*, 193−194.
(39) Cantor, C. R.; Warshaw, M. M.; Shapiro, H. *Biopolymers* **1970**, *9*, 1059−1077.
(40) Fasman, G. D. *Optical Properties of Nucleic Acids, Absorption, and circular dichroism spectra*, 3rd ed.; CRC Press: Cleveland, OH, 1975; Vol. 1, p 58.
(41) Wei, M.; Cohen, S. M.; Silverman, A. P.; Lippard, S. J. *J. Biol. Chem.* **2001**, *276*, 38774−38780.

with T4 polynucleotide kinase under standard conditions. A 500 pmol quantity of each appropriate phosphorylated strand, 1000 pmol of one of the 14-mers **d1**, **d1-Pt**, **d2**, or **d2-Pt**, and the oligonucleotides **a** and **e** were annealed in buffer (100 mM NaCl, 70 mM Tris/HCl, pH 7.5, 10 mM $MgCl_2$) by applying a temperature gradient from 90 °C to 4 °C over 3 h and ligated *in situ* (50 mM NaCl, 60 mM Tris/HCl, 10 mM $MgCl_2$, 10 mM DTT, 1.5 mM ATP, 25 μg/mL BSA, 10 U/μL T4 DNA ligase, 48 h, 16 °C) to give the duplex DNAs **S1, S1-Pt, S2**, and **S2-Pt** detailed in Scheme 1 (sequences in Scheme S1c, Supporting Information). The sample strands were then phenol extracted, ethanol precipitated twice, and purified on a 6% denaturing polyacrylamide gel. Under these conditions, the duplexes dissociated and it was possible to separate completely the 145-bp template strands from the 154-bp coding strands. The ligation reaction itself proceeded quantitatively, with isolated yields of the single strands (UV/vis) varying between 38% and 50%. The resulting single strands were analyzed by a modified Maxam−Gilbert A/G reaction[42] to confirm the sequence and position of the cisplatin adducts. Before electrophoretic analysis of the Maxam−Gilbert fragments, the samples were treated with 0.2 M KCN at 50 °C overnight to remove the platinum adduct. Residual KCN was separated by ethanol precipitation and redissolution of the DNA. This procedure removed DNA-bound cisplatin completely, resulting in a significantly increased resolution of the sequencing reactions (Figure S5, Supporting Information). Aligned profiles of the Maxam−Gilbert traces were generated with the program SAFA V1.1,[43] which is available free of charge from http://safa.stanford.edu. Approximately 120 bands were resolved that corresponded to the designed sequence. The position of the cisplatin lesion was identified by the missing double bands in the platinated samples when compared to the corresponding unplatinated reference strands.

For histone transfer reactions, a 15 pmol quantity of either the template strands or coding strands was labeled with 250 μCi γ-^{32}P-ATP per reaction by using T4 polynucleotide kinase (37 °C, 2 h). The reaction was terminated by addition of 500 pmol of EDTA, and the enzyme was heat deactivated. Unreacted γ-^{32}P-ATP was removed with a MicroSpin G-25 gel filtration cartridge (Amersham) and the DNA concentrated by ethanol precipitation. Smaller DNA fragments that are formed due to autoradiolysis during the labeling reaction were then removed by preparative PAGE in the presence of 7.5 M urea. The purified labeled DNA was then combined with an approximately equimolar amount of the appropriate complementary strand, and residual urea was removed with a ProbeQuant G-50 gel filtration cartridge (Amersham). The salt concentration was brought to 150 mM NaCl, 1 mM EDTA-Na_2, and 10 mM Tris/HCl, and the DNA was annealed by applying a temperature gradient from 90 °C to 20 °C over 3 h. The labeled duplexes were further purified by native PAGE (6% w/w polyacrylamide) to remove any excess single-stranded DNA. Single-end radiolabeled ($2-5 \times 10^6$ cpm), highly purified duplex DNA was obtained, which was stored frozen at concentrations no higher than 2×10^4 cpm/μL to reduce nicking by autoradiolysis.

Nucleosome Reconstitution. A 5×10^6 cpm quantity of **S1**, **S1-Pt**, **S2**, or **S2-Pt** (5′-labeled with ^{32}P as described above, on either the template or coding strand) was combined with donor chromatin from HeLa-S3 cells[44] having an average length of 2−3 nucleosomes. The reaction was brought to 50 μL in 10 mM Tris, 2 M NaCl, 5 mM DTT, 0.5 mM PMSF, 0.2 mM EDTA, 0.01% (v/v) Nonidet-P40, pH 7.5, and dialyzed for 2 days in microdialysis buttons that were constructed from the cap of a 500 μL polymerase chain reaction tube and a 1 cm^2 Spectra/Por MWCO 6−8 kDa dialysis membrane.[45] The membrane was treated with EDTA and soaked in a 2 M NaCl solution prior to use. The buttons were first dialyzed at 4 °C for 1 h against 20 mL of a high-salt buffer, TB-1, containing 10 mM Tris, 2 M NaCl, 1 mM DTT, 0.5 mM PMSF, and 0.01% (v/v) Nonidet-P40 at pH 7.5. The buffer TB-1 was transferred together with the buttons into a secondary dialysis tube (Spectra/Por MWCO 6−8 kDa). The secondary tube was dialyzed against 1.5 L of a low-salt buffer, TB-2 (10 mM Tris, 0.2 mM PMSF, pH 7.5, 4 °C), overnight. The samples were recovered from the dialysis buttons and equilibrated at 45 °C for 2 h.

Hydroxyl Radical Footprinting of Nucleosomes. Hydroxyl radical footprinting[26] and nucleosome purification were performed as follows. A 7.5 μL aliquot of 10 mM sodium ascorbate, 7.5 μL of a solution containing 1 mM $Fe(NH_4)_2(SO_4)_2 \cdot 6H_2O$ and 2 mM EDTA, and 7.5 μL of a 0.12% (w/w) H_2O_2 solution were premixed and added within 5 s to 52.5 μL of the nucleosome sample. The reaction was incubated for 120 s at room temperature and stopped by addition of 8 μL of 50% (v/v) glycerol and 2 μL of a 500 mM EDTA solution. The samples were immediately loaded onto a cooled 4.5% native gel (37.5:1 acrylamide/bisacrylamide, thickness 1.6 mm, 0.3 × TBE) and run for 4 h at 100 V. The gel was wrapped in plastic and exposed to a Biomax MS film for 30 min. The bands were cut out using the exposed film as a template (Figure S6, Supporting Information). The nucleosomes were isolated from the gel by electroelution with a Millipore Centrilutor Microeluter system into Centricon 3 K microfiltration cartridges (0.3 × TBE, 200 V, 2 h). The sample volumes were reduced, and the buffer was exchanged against 300 μL of TE buffer by centrifugation. The histones were digested afterward by treatment with 20 ng/mL of Proteinase K and 0.1% (w/v) SDS for 3 h at 50 °C and removed by two subsequent phenol extractions. Residual phenol was then removed by ether extraction followed by ethanol precipitation. The pellets were dissolved in 40 μL of 0.2 M KCN and shaken at 50 °C overnight to remove the platinum adduct. The samples were then ethanol precipitated twice, and the pellet was rinsed with 70% ethanol. The purified DNA was finally taken up in TE buffer and stored at 5 °C. Typically, $(2-5) \times 10^5$ cpm of radiolabeled DNA was recovered. As a reference, hydroxyl radical footprinting was also conducted with all unbound sample duplexes **S1**, **S1-Pt**, **S2**, and **S2-Pt**. A 2×10^5 cpm quantity of the single-end-labeled duplexes, labeled on either the template or the coding strand, was brought to a volume of 35 μL. A 5 μL portion of 10 mM sodium ascorbate, 5 μL of a solution containing 1 mM $Fe(NH_4)_2(SO_4)_2 \cdot 6H_2O$ and 2 mM EDTA, and 5 μL of a 0.12% (w/w) H_2O_2 solution were premixed and added within 5 s to the sample. After incubation for 120 s, 20 μL of a stop solution containing 1 M sodium acetate, 120 mM thiourea, 300 μg/mL salmon sperm DNA, and 60 mM EDTA at pH 6.5 was added. The samples were ethanol precipitated and treated with KCN as described above. The DNA was precipitated twice and then rinsed with 70% ethanol. The pellets were taken up in TE buffer and stored at 5 °C. A 3×10^4 cpm aliquot of each footprinting sample was pipetted into new reaction tubes and completely dried by vacuum centrifugation. The dried samples were taken up in 2.5 μL of freshly deionized formamide containing 10 mM EDTA and heated to 90 °C for 120 s. Immediately after heating, the samples were cooled on ice and loaded onto an 8% denaturing sequencing gel (0.4 mm thickness, 25:1 acrylamide/bisacrylamide, 7.5 M urea, 1 × TBE). The electrophoresis was run for 2−3 h at 65 W until the bromphenol blue marker (run in an extra lane) was about 4 cm above the bottom edge of the gel. Gels were blotted onto Whatman paper, dried, and exposed for 3 days to a phosphorscreen.

Data Collection and Processing. The gel images were processed by the footprinting analysis software SAFA V1.1.[43] The gel was first horizontally and vertically aligned with help of this software. Next, each band of the Maxam−Gilbert reference lane was aligned with the known DNA sequence. The program uses this information as a starting guess to conduct a least-squares fit of a sum of Lorentzians to the intensity profiles derived from the footprinting data. Each identified band was assigned a relative value derived by integration of the fitted Lorentzian. The individual values are shown in Table S1 (Supporting Information). Cleavage curves were calculated from these values by

(42) Ambrose, B. J. B.; Pless, R. C. *Methods Enzymol.* **1987**, *152*, 522−538.
(43) Das, R.; Laederach, A.; Pearlman, S. M.; Herschlag, D.; Altman, R. B. *RNA* **2005**, *11*, 344−354.
(44) Utley, R. T.; Owen-Hughes, T. A.; Juan, L. J.; Côté, J.; Adams, C. C.; Workman, J. L. *Methods Enzymol.* **1996**, *274*, 276−291.
(45) Thåström, A.; Lowary, P. T.; Widom, J. *Methods* **2004**, *33*, 33−44.

applying a moving average with a window of 5 bp. The aligned densitometric profiles (Figures S3 and S4, Supporting Information) were also determined with SAFA. Wavelength demodulation of the cleavage curves (Figure 7) and determination of helical periodicities were performed as follows. For every nucleosome, the *x*-values of the maxima of the cleavage curve were determined (max_i). The distances between two consecutive maxima, $y = max_i - max_{i-1}$, were plotted against the mean value of these maxima, $x = (max_i + max_{i-1})/2$. Minima were processed in the same way. Points obtained for the extrema of both single strands of one duplex were combined in one graph. The data were smoothed by applying a moving average with a window of 5. Mean periodicities per nucleosome were calculated as $[\sum_{a=1}^{i-1}(max_{a+1} - max_a) + \sum_{b=1}^{k-1}(min_{b+1} - min_b)]/(i + k - 2)$, with i being the total number of observed maxima and k the total number of minima identified in each cleavage curve. In order to determine the location of the major and minor grooves of the duplex DNA, the cleavage curves of both strands of the nucleosomal DNA duplex were superimposed. Next, the *x*-distances between every maximum of one strand and the two neighboring maxima of the complementary strand were determined. The areas between nearer maxima indicate where the minor groove was exposed to solvent on the nucleosome surface. At the remaining locations, the major groove is solvent-exposed. All traces were consistently color-coded according their sequence as follows: **S1**, blue; **S1-Pt**, red; **S2**, green; **S2-Pt**, orange/brown.

Acknowledgment. This work was generously supported by NIH grant CA34992. M.O. thanks the Alexander von Humboldt Foundation, Germany, for support through a Feodor-Lynen Fellowship.

Supporting Information Available: Sequences of DNA strands and sample duplexes, enlarged versions of the autoradiographs, densitometric scans of footprinting reactions and sequence alignment, Maxam−Gilbert sequencing analysis of duplexes, chromatin preparation from HeLa-S3 cells, details about histone transfer reactions, nucleosome purification, definition of the angle ξ, and tables of deconvoluted ^{32}P signals and helical periodicities. This material is available free of charge via the Internet at http://pubs.acs.org.

JA0706145